

experimentation; nevertheless, two of the more straightforward mechanistic possibilities can be briefly considered. The first involves covalent solvation²⁵ of the coordinated dmp ligands. Such solvation has, for example, been proposed to rationalize the solution photophysics of bipyridine.²⁶ (But see also ref 27.) If covalent solvation has any significance for the ligands of $[\text{Cu}(\text{dmp})_2]^+$, however, it probably cannot explain the results for all quenchers, since the interaction seems improbable for acetonitrile.

A second phenomenon—coordination at the metal center—is an intriguing alternative. One obvious property that the alcohols and acetonitrile have in common is their Lewis basicity. Since the metal center is formally Cu(II) in the $d-\pi^*$ excited state, the addition of a fifth donor group about the metal is possible. In fact it has been proposed²⁸ that solvent and/or counterions do associate with the (ground state) Cu(II) analogue $[\text{Cu}(\text{dmp})_2]^{2+}$. Moreover, coordination numbers of 5 and 6 are well established for related phenanthroline²⁹ and bipyridine complexes³⁰ of Cu(II). That an excited state may be capable of exhibiting an expanded coordination number has previously been suggested in the case of certain Cr(III) systems.³¹ In addition, in a recent structural report it was noted

that the Cr(III) center in the bis(terpyridyl) complex is rather exposed, and it was suggested that solvent interactions with the metal center may be responsible for the short excited-state lifetime of the complex.³²

Conclusions

Strong evidence for a reactive charge-transfer excited state of $[\text{Cu}(\text{dmp})_2]^+$ has been obtained from emission quenching studies in CH_2Cl_2 . The excited state is strongly reducing, and most of the excited state energy seems to be available as electrochemical potential. Donor solvents appear to quench the emission, possibly by interaction at the metal center. CH_2Cl_2 may be a good solvent for use in photostudies of complexes exhibiting relatively "exposed" metal centers; however, it should be emphasized that CH_2Cl_2 can undergo reaction with excited molecules³³ and can influence the reactivity of excited molecules.³⁴

Acknowledgment. The authors gratefully acknowledge the Atlantic Richfield Foundation which has helped fund our work through a contribution to the Research Corp. They also thank Richard J. Watts, who provided the lifetime measurement and a corrected emission spectrum of $[\text{Ru}(\text{bpy})_3]^{2+}$.

Registry No. $[\text{Cu}(\text{dmp})_2]^+$, 21710-12-3.

- (25) Gillard, R. D. *Coord. Chem. Rev.* **1975**, *16*, 67.
 (26) Henry, M. S.; Hoffman, M. Z. *J. Phys. Chem.* **1979**, *83*, 618.
 (27) Kotlicka, J.; Grabowski, Z. R. *J. Photochem.* **1979**, *11*, 413.
 (28) (a) Hall, J. R.; Marchant, N. K.; Plowman, R. A. *Aust J. Chem.* **1963**, *16*, 34. (b) Rehorek, D. Z. *Chem.* **1978**, *18*, 32. (c) Sundararajan, S.; Wehry, E. L. *J. Inorg. Nucl. Chem.* **1972**, *34*, 3699.
 (29) (a) Nakai, H.; Noda, Y. *Bull. Chem. Soc. Jpn.* **1978**, *51*, 1386. (b) Anderson, O. P. *Inorg. Chem.* **1975**, *14*, 730.
 (30) (a) Barklay, G. A.; Hoskins, B. F.; Kennard, C. H. L. *J. Chem. Soc.* **1963**, 5691. (b) Stephens, F. S. *J. Chem. Soc., Dalton Trans.* **1972**, 1350. (c) Proctor, J. M.; Stephens, F. S. *J. Chem. Soc. A* **1969**, 1248.

- (31) (a) Sandrini, D.; Gandolfi, M. T.; Juris, A.; Balzani, V. *J. Am. Chem. Soc.* **1977**, *99*, 4523. (b) Jamieson, M. A.; Serpone, N.; Henry, M. S.; Hoffman, M. Z. *Inorg. Chem.* **1979**, *18*, 214.
 (32) Wickramasinghe, W. A.; Bird, P. H.; Jamieson, M. A.; Serpone, N. *J. Chem. Soc., Chem. Commun.* **1979**, 798.
 (33) (a) Saperstein, D.; Levin, E. *J. Chem. Phys.* **1979**, *62*, 3560. (b) Felt, G. R.; Linke, S.; Lwowski, W. *Tetrahedron Lett.* **1972**, 2037.
 (34) (a) Gleria, M.; Minto, F.; Beggato, G.; Bortolus, P. *J. Chem. Soc., Chem. Commun.* **1977**, 285. (b) Durham, B.; Walsh, J. L.; Carter, C. L.; Meyer, T. J. *Inorg. Chem.* **1980**, *19*, 860.

Contribution from the Christopher Ingold Laboratories, University College, London WC1H 0AJ, United Kingdom

Electronic and Resonance Raman Spectra of Mixed-Valence Linear-Chain Complexes of Platinum with 1,3-Diaminopropane

ROBIN J. H. CLARK* and MOHAMEDALLY KURMOO

Received February 29, 1980

The resonance Raman spectra of mixed-valence complexes $[\text{Pt}(\text{tn})_2][\text{Pt}(\text{tn})_2\text{X}_2]\text{Y}_4$ (tn = 1,3-diaminopropane, X = Cl, Br, or I for Y = ClO_4 , and X = Br for Y = BF_4) have been recorded at ca. 80 K by use of excitation lines whose wavenumbers fall within the contours of the intense, axially polarized intervalence bands of each complex. The resonance Raman and specular reflectance spectra of a single crystal of $[\text{Pt}(\text{tn})_2][\text{Pt}(\text{tn})_2\text{Br}_2](\text{ClO}_4)_4$ have also been recorded, at room temperature. The resonance Raman spectra are characterized by the appearance of an intense progression $\nu_1\nu_1$, where ν_1 is the symmetric (X-Pt^{IV}-X) stretching mode. The maximum value of ν_1 ranges from 4 to 18. Other short progressions, $\nu_n + \nu_1\nu_1$, based on other Raman-active modes, have also been observed. From the observed progressions the spectroscopic constants ω_1 and x_{11} have been calculated. The specular reflectance and polarized Raman spectra from single crystals show semiconductor behavior in one direction. The excitation profiles of ν_1 (both Stokes and anti-Stokes bands), $2\nu_1$ (Stokes bands), and (in some cases) $3\nu_1$ (Stokes bands) all maximize within 500 cm^{-1} of each other, and all on the low wavenumber side of the resonant mixed-valence band in each case.

Introduction

Previous studies in this series on mixed-valence complexes of platinum and palladium, belonging to Class II in the Robin and Day¹ scheme, have been focused on complexes containing ethylamine,²⁻⁴ ammonia,⁵ 1,2-diaminopropane,⁶ and 1,2-di-

aminoethane.⁷ The present paper develops this subject further and is concerned with platinum complexes with 1,3-diaminopropane (tn), $[\text{Pt}(\text{tn})_2][\text{Pt}(\text{tn})_2\text{X}_2]\text{Y}_4$ (X = Cl, Br, or I for Y = ClO_4 and X = Br for Y = BF_4). This ligand, which forms a six-membered aliphatic ring with the metal atom, appears to form linear-chain complexes with as much facility as is found for monodentate amines and for other bidentate amines capable of forming five-membered aliphatic rings with the metal atom. The results obtained add substantially to the body

- (1) Robin, M. B.; Day, P. *Adv. Inorg. Chem. Radiochem.* **1968**, *10*, 247.
 (2) Clark, R. J. H.; Franks, M. L.; Trumble, W. R. *Chem. Phys. Lett.* **1976**, *41*, 287.
 (3) Clark, R. J. H.; Franks, M. L. *J. Chem. Soc., Dalton Trans.* **1977**, 198.
 (4) Clark, R. J. H.; Turtle, P. C. *Inorg. Chem.* **1978**, *17*, 2526.
 (5) Clark, R. J. H.; Turtle, P. C. *J. Chem. Soc., Dalton Trans.* **1979**, 1622.
 (6) Clark, R. J. H.; Stewart, B. *Struct. Bonding (Berlin)* **1979**, *36*, 1.

- (7) Campbell, J. R.; Clark, R. J. H.; Turtle, P. C. *Inorg. Chem.* **1978**, *17*, 3623.

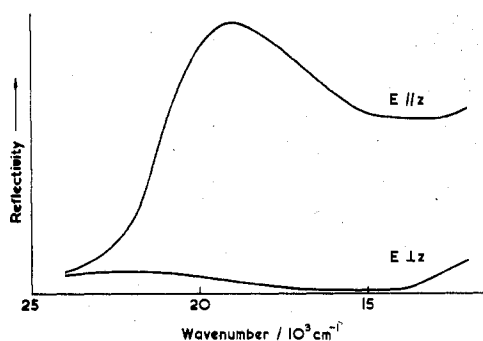


Figure 1. Single-crystal reflectance spectra of $[\text{Pt}(\text{tn})_2][\text{Pt}(\text{tn})_2\text{Br}_2](\text{ClO}_4)_4$ with $E \parallel Z$ and $E \perp Z$.

of information on this class of complex, which occupy a position as intrinsic semiconductors intermediate between insulators such as K_2PtCl_4 and one-dimensional metals such as $\text{KCP}, \text{K}_2\text{Pt}(\text{CN})_4 \cdot \text{Br}_{0.30} \cdot 3\text{H}_2\text{O}$.

The structures of these complexes consist of infinite chains⁸ of $\text{X}-\text{Pt}^{\text{IV}}-\text{X} \cdots \text{Pt}^{\text{II}}$ units parallel to each other with $[\text{Pt}(\text{tn})_2]^{2+}$ in square-planar coordination and $[\text{Pt}(\text{tn})_2\text{X}_2]^{2+}$ in tetragonal-bipyramidal coordination. The $\text{Pt}^{\text{IV}}-\text{X}/\text{Pt}^{\text{II}}-\text{X}$ bond length ratio increases in the order $\text{Cl} < \text{Br} < \text{I}$, indicating a tendency in this order to a $\text{Pt}(\text{III})$ -type complex. This is consistent with the X-ray photoelectron⁹ experiments on the $[\text{Pt}(\text{en})_2][\text{Pt}(\text{en})_2\text{X}_2](\text{ClO}_4)_4$ complexes (where $\text{X} = \text{Cl}, \text{Br}, \text{or I}$).

Some room-temperature resonance Raman (RR) spectra of the bromo complexes¹⁰ consist of a progression in ν_1 , the $\nu(\text{X}-\text{Pt}^{\text{IV}}-\text{X})$ breathing mode, reaching as far as 5 members in each case. The present results, obtained at ca. 80 K, are far more detailed than these, $\nu_1\nu_1$ progressions being shown to reach a maximum of $\nu_1 = 18$, and they allow various spectroscopic constants to be calculated with considerable accuracy.

Experimental Section

$[\text{Pt}(\text{tn})_2][\text{Pt}(\text{tn})_2\text{X}_2]\text{Y}_4$ ($\text{X} = \text{Cl}$ or Br) were obtained by the method of Kida,¹¹ using H_2PtCl_6 for the chloride and K_2PtBr_6 for the bromide. The iodo complex was obtained by the method of Bekaroglu et al.¹² Recrystallizations were carried out from dilute perchloric or fluoroboric acids. Single crystals were grown by slow cooling of saturated aqueous solutions.

Electronic spectra were obtained from pressed disks of the complexes dispersed in KClO_4 or alkali halide by using a Cary 14 spectrometer. Specular reflectance spectra of single crystals were recorded on a Spex 1000 monochromator.

Infrared spectra were obtained from Nujol mulls of the complexes by using a Perkin-Elmer 225 spectrometer.

Raman spectra were recorded by using Spex 1401 or 14018 (R6) double/triple monochromators equipped with standard photon-counting detection systems. Exciting radiation was provided by Coherent Radiation Models 52 and 12 Ar^+ and 52 Kr^+ lasers. Raman spectra at room temperature were obtained by using the rotating-sample method¹³ and at ca. 80 K by the flicking-laser-beam method.⁴ The spectra were calibrated by using neon emission lines. Excitation profile measurements were made at room temperature with respect to the ν_1 band of SO_4^{2-} or ClO_4^- as standards and corrected for the spectral response of the instrument. All complexes were found to analyze satisfactorily for C, H, N, and halogen.

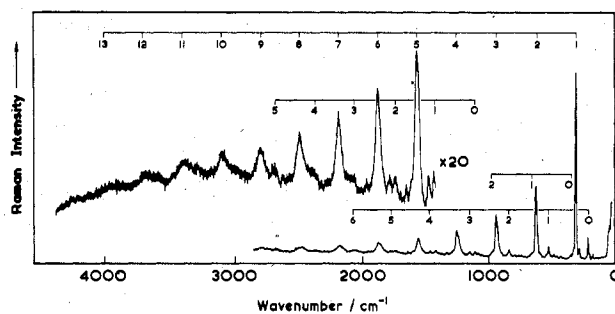


Figure 2. Resonance Raman spectrum of $[\text{Pt}(\text{tn})_2][\text{Pt}(\text{tn})_2\text{Cl}_2](\text{ClO}_4)_4$ in a KClO_4 disk at ca. 80 K ($\lambda_0 = 482.5$ nm, slit width ≈ 1.5 cm^{-1}).

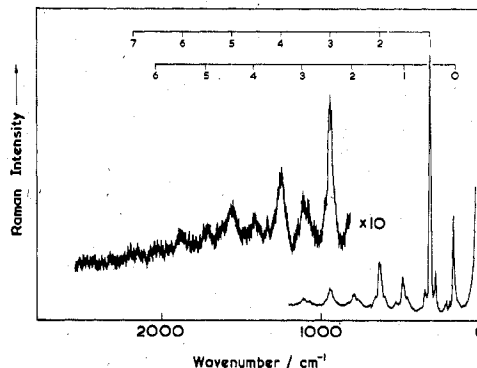


Figure 3. Resonance Raman spectrum of $[\text{Pt}(\text{tn})_2][\text{Pt}(\text{tn})_2\text{Cl}_2](\text{ClO}_4)_4$ in a CsCl disk at ca. 80 K, after exposure to moist air ($\lambda_0 = 457.9$ nm, slit width ≈ 2.0 cm^{-1}).

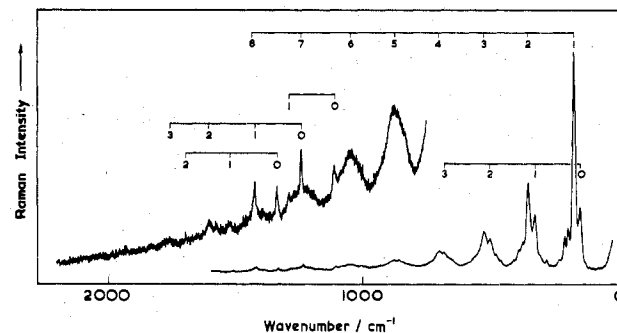


Figure 4. Resonance Raman spectrum of $[\text{Pt}(\text{tn})_2][\text{Pt}(\text{tn})_2\text{Br}_2](\text{ClO}_4)_4$ in a KClO_4 disk at ca. 80 K ($\lambda_0 = 568.2$ nm, slit width ≈ 2.0 cm^{-1}).

Electronic Spectra

The crystals of these complexes show remarkable dichroism. The chlorides are dark red for radiation polarized along the needle axis and colorless for that polarized perpendicular to this axis. The bromides are dark green for radiation parallel to and light yellow for that perpendicular to this axis, and the iodide is dark blue and yellow, respectively. Specular reflectance spectra of $[\text{Pt}(\text{tn})_2][\text{Pt}(\text{tn})_2\text{X}_2](\text{ClO}_4)_4$ ($\text{X} = \text{Br}$ or I) show¹⁴ a broad band in the visible-near IR region, with the electric vector of the incident light beam parallel to the conducting axis ($E \parallel Z$) and no absorption when the electric vector is perpendicular to the axis ($E \perp Z$). Figure 1 shows the reflectance spectra of the bromide for the two polarizations.

Since these complexes change color when ground with alkali halide and exposed to the atmosphere, the electronic spectra were recorded in two matrices, namely, KClO_4 and the appropriate alkali halide. Table I lists the electronic band maxima and the matrices. These broad bands are assigned to the intervalence bands of the type $\text{Pt}^{\text{IV}}(d_2) \leftarrow \text{Pt}^{\text{II}}(d_2)$.

(8) Matsumoto, N.; Yamashita, M.; Kida, S. *Bull. Chem. Soc. Jpn.* **1978**, *51*, 3514.

(9) Yamashita, M.; Matsumoto, N.; Kida, S. *Inorg. Chim. Acta* **1978**, *31*, L381.

(10) Ohta, N.; Kozuka, M.; Nakamoto, K.; Yamashita, M.; Kida, S. *Chem. Lett.* **1978**, 843.

(11) Kida, S. *Bull. Chem. Soc. Jpn.* **1965**, *38*, 1804.

(12) Bekaroglu, O.; Breer, H.; Endres, H.; Keller, H. J.; Gung, N. H. *Inorg. Chim. Acta* **1977**, *21*, 183.

(13) Kiefer, W. In "Advances in Infrared and Raman Spectroscopy"; Clark, R. J. H., Hester, R. E., Eds.; Heyden: London, 1977; Vol. 3, p 1.

(14) Bloor, D.; Clark, R. J. H.; Kurmoo, M.; Kennedy, R., unpublished work.

Table I. Summary of Data on Complexes Studied

complex	crystal ^a	powder	disk matrix	disk color	mixed-valence band max, cm ⁻¹ b	excitation profile (ν_1) max, cm ⁻¹	ω_1 , cm ⁻¹	x_{11} , cm ⁻¹	pro- gression (80 K) ^c	$I(2\nu_1)/I(\nu_1)_{\max}$	Pt ^{IV} -X, Å	Pt ^{II} -X, Å
[Pt(tn) ₂][Pt(tn) ₂ Cl ₂](ClO ₄) ₄	red needles	red	KClO ₄	pink	22 900	18 600	315.0 ± 0.30	-0.71 ± 0.04	13 ν_1	0.64	2.299 ^d	3.096 ^d
[Pt(tn) ₂][Pt(tn) ₂ Br ₂](ClO ₄) ₄	green-gold needles	blue	CsCl KClO ₄	yellow ^e blue	25 200 18 400	≥22 000 ≤12 500, 17 600 ^f	317.8 ± 0.70 181.2 ± 0.50	-0.71 ± 0.15 -1.04 ± 0.12	8 ν_1 8 ν_1	0.31 0.50	2.546	2.955
[Pt(tn) ₂][Pt(tn) ₂ Br ₂](BF ₄) ₄	green-gold needles	blue	K ₂ SO ₄ KBr	blue reddish	14 000 21 500		≈178 ≈184		12 ν_1 8 ν_1	0.52 0.59	2.541	2.921
[Pt(tn) ₂][Pt(tn) ₂ I ₂](ClO ₄) ₄	gold needles	blue	KClO ₄ CsI	blue brown ^e	13 500 24 900	≤12 500 18 800	131.4 ± 0.9 127.2 ± 0.70	0.1 ± 0.3 -0.2 ± 0.2	4 ν_1 5 ν_1	0.48 0.39	Pt ^{IV} -I/Pt ^{II} -I ≈0.90	

^a By reflected light. ^b By transmission, giving effectively the sum of ϵ_{\parallel} and ϵ_{\perp} . ^c ν_1 is the $\nu_{\text{sym}}(\text{X}-\text{Pt}^{\text{IV}}-\text{X})$ fundamental. ^d BF₄ salt. ^e The colors of the complexes in alkali halide disks are identical with those in KClO₄ or K₂SO₄ disks if the alkali halide is dry (see text). ^f Shoulder.

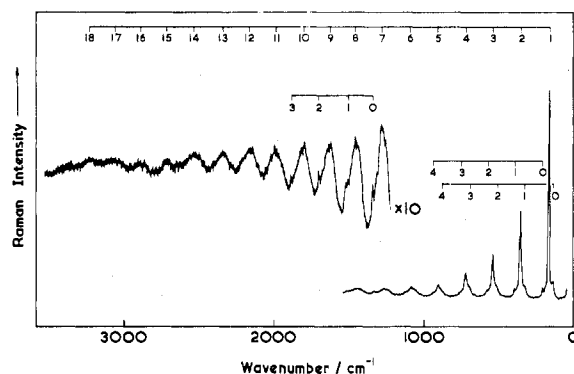


Figure 5. Resonance Raman spectrum of [Pt(tn)₂][Pt(tn)₂Br₂](ClO₄)₄ in a KBr disk at ca. 80 K, after exposure to moist air ($\lambda_0 = 488.0$ nm, slit width ≈ 1.5 cm⁻¹).

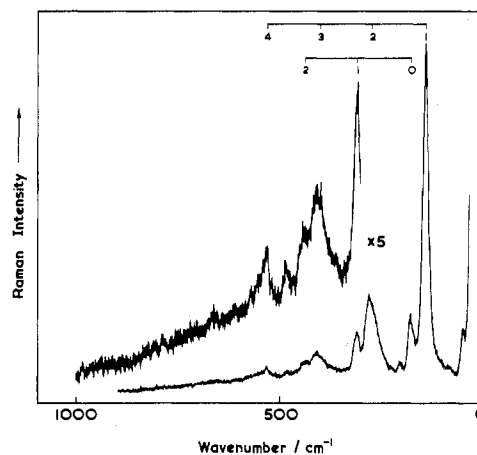


Figure 6. Resonance Raman spectrum of [Pt(tn)₂][Pt(tn)₂I₂](ClO₄)₄ in a KClO₄ disk at ca. 80 K ($\lambda_0 = 676.4$ nm, slit width ≈ 3.0 cm⁻¹).

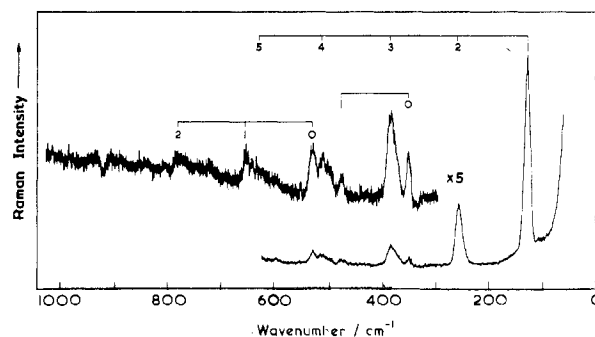


Figure 7. Resonance Raman spectrum of [Pt(tn)₂][Pt(tn)₂I₂](ClO₄)₄ in a CsI disk at ca. 80 K, after exposure to moist air ($\lambda_0 = 488.0$ nm, slit width ≈ 5.0 cm⁻¹).

Since the wavenumbers of the band maxima decrease in the order Cl > Br > I, it is assumed that the charge-transfer involves the s and p orbitals of the halides in the chains.

Resonance Raman Spectra

The RR spectra of the complexes at ca. 80 K are shown in Figures 2–7, and the wavenumbers and assignments of the bands observed are listed in Tables II–IV. RR spectra obtained with excitation whose wavenumber falls within the contours of the intervalence bands show long progressions in ν_1 , the symmetric (X–Pt^{IV}–X) stretching mode. The band maxima associated with the progressions in ν_1 are listed in Table I for each complex in the two matrices at ca. 80 K.

Single-crystal polarized RR spectra of the complex [Pt(tn)₂][Pt(tn)₂Br₂](ClO₄)₄ show a progression to 5 ν_1 (at ca. 298 K) for the electric vector of the incident light parallel to the

Table II. Wavenumbers (cm^{-1}) of Bands Observed in the Resonance Raman Spectrum of $[\text{Pt}(\text{tn})_2][\text{Pt}(\text{tn})_2\text{Cl}_2](\text{ClO}_4)_4$ at Ca. 80 K

KClO_4^a		
153.1	1414	$\nu_3 + \nu_1$
184.2	1467	$\nu_2 + 4\nu_1$
202.7	1554	$5\nu_1$
216.7	1643	$\nu_4 + \nu_1$
255.1	1733	$\nu_3 + 2\nu_1$
285.8	1778	$\nu_2 + 5\nu_1$
312.9	1862	$6\nu_1$
351.9	1953	$\nu_4 + 2\nu_1$
432.6	2046	$\nu_3 + 3\nu_1$
485.0	2087	$\nu_2 + 6\nu_1$
530.3	2170	$7\nu_1$
548.0	2351	$\nu_3 + 4\nu_1$
599.6	2473	$8\nu_1$
626.6	2654	$\nu_3 + 5\nu_1$
663.0	2767	$9\nu_1$
749.0	2997	$\nu_3 + 6\nu_1$
841.9	3068	$10\nu_1$
936.9	3367	$11\nu_1$
1108.3	3642	$12\nu_1$
1153.4	3922	$13\nu_1$
1244.4		
1327.7		
	CsCl^b	
172.6	801.2	$\nu_3 + 2\nu_1$
214.0	947.8	$3\nu_1$
284.0	1105	$\nu_3 + 3\nu_1$
315.2	1257.5	$4\nu_1$
348.8	1362	$\nu_4, \delta(\text{H-C-H})$
456.4	1425	$\nu_3 + 4\nu_1$
486.0	1565	$5\nu_1$
532.4	1725	$\nu_3 + 5\nu_1$
604.4	1875	$6\nu_1$
632.8	2045	$\nu_3 + 6\nu_1$
665.6	2185	$7\nu_1$
766.4	2475	$8\nu_1$

^a Obtained at ca. 80 K as a KClO_4 disk with 482.5-nm excitation. ^b Obtained at ca. 80 K as a CsCl disk with 457.9-nm excitation, after exposure to moist air.

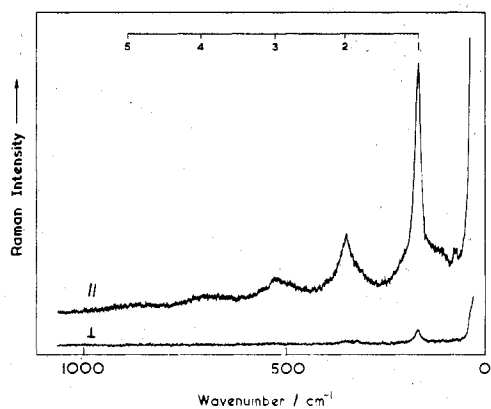


Figure 8. Resonance Raman spectra of a single crystal of $[\text{Pt}(\text{tn})_2][\text{Pt}(\text{tn})_2\text{Br}_2](\text{ClO}_4)_4$ at ca. 298 K with $\text{E}||\text{Z}$ and the analyzer perpendicular to Z and parallel to Z ($\lambda_0 = 568.2$ nm, slit width ≈ 4 cm^{-1}).

conducting axis ($\text{E}||\text{Z}$) and no bands for the electric vector perpendicular to this axis ($\text{E}\perp\text{Z}$). The RR spectra for the two polarizations are shown in Figure 8. This shows the one-dimensional properties typical of this type of the complex and that the progression-forming mode is totally symmetric.

The RR spectra of these complexes also display weak subsidiary progressions $\nu_n + \nu_1$ in which ν_1 is the progression-forming mode and ν_n is another Raman-active mode. The wavenumbers and assignments of these bands are listed in Tables II–IV, and the great length of the RR progressions is

Table III. Wavenumbers (cm^{-1}) of Bands Observed in the Resonance Raman Spectrum of $[\text{Pt}(\text{tn})_2][\text{Pt}(\text{tn})_2\text{Br}_2](\text{ClO}_4)_4$ at Ca. 80 K

KClO_4^a		
153.8	ν_2	686.2 $\nu_2 + 3\nu_1$
178.8	$\nu_1, \nu(\text{Br-Pt}^{\text{IV}}-\text{Br})$	706.2 $4\nu_1$
200.4		871 $5\nu_1$
214.2		1039 $6\nu_1$
236.7		1105 $\nu_3, \nu(\text{C-N})$
285.4		1215 $7\nu_1$
330.0	$\nu_2 + \nu_1$	1235 ν_5
356.8	$2\nu_1$	1285 $\nu_3 + \nu_1$
379.8	$\nu_1 + 200.4$	1327 $\nu_4, \delta(\text{H-C-H})$
394.7	$\nu_1 + 214.2$	1416 $8\nu_1/\nu_5 + \nu_1$
466.2	$\nu_1 + 285.4$	1508 $\nu_4 + \nu_1$
481.2		1593 $\nu_5 + 2\nu_1$
509.6	$\nu_2 + 2\nu_1$	1688 $\nu_4 + 2\nu_1$
531.5	$3\nu_1$	1754 $\nu_5 + 3\nu_1$
	KBr^b	
153.7	ν_2	1341 $\nu_4, \delta(\text{H-C-H})$
183.1	$\nu_1, \nu(\text{Br-Pt}^{\text{IV}}-\text{Br})$	1459 $8\nu_1$
220.7		1522 $\nu_4 + \nu_1$
337.5	$\nu_2 + \nu_1$	1640 $9\nu_1$
366.8	$2\nu_1$	1703 $\nu_4 + 2\nu_1$
404.3	$\nu_1 + 220.7$	1821 $10\nu_1$
521.9	$\nu_2 + 2\nu_1$	1884 $\nu_4 + 3\nu_1$
549.9	$3\nu_1$	2002 $11\nu_1$
586.3	$2\nu_1 + 220.7$	2183 $12\nu_1$
705.3	$\nu_2 + 3\nu_1$	2364 $13\nu_1$
732.8	$4\nu_1$	2545 $14\nu_1$
771.9	$3\nu_1 + 220.7$	2726 $15\nu_1$
887.5	$\nu_2 + 4\nu_1$	2907 $16\nu_1$
914.9	$5\nu_1$	3088 $17\nu_1$
1096.8	$6\nu_1$	3270 $18\nu_1$
1277.8	$7\nu_1$	

^a Obtained at ca. 80 K as a KClO_4 disk with 568.2-nm excitation. ^b Obtained at ca. 80 K as a KBr disk with 488.0-nm excitation, after exposure to moist air.

Table IV. Wavenumbers (cm^{-1}) of Bands Observed in the Resonance Raman Spectrum of $[\text{Pt}(\text{tn})_2][\text{Pt}(\text{tn})_2\text{I}_2](\text{ClO}_4)_4$ at Ca. 80 K

KClO_4^a		
131.0	$\nu_1, \nu(\text{I-Pt}^{\text{IV}}-\text{I})$	396.1 $3\nu_1$
167.3	ν_2	430.6 $\nu_2 + 2\nu_1$
264.9	$2\nu_1$	526.0 $4\nu_1$
297.3	$\nu_2 + \nu_1$	
	CsI^b	
126.1	$\nu_1, \nu(\text{I-Pt}^{\text{IV}}-\text{I})$	505.5 $4\nu_1$
254.5	$2\nu_1$	528.7 $\nu_3, \nu(\text{Pt-N})$
346.3	ν_2	628.7 $5\nu_1$
381.6	$3\nu_1$	656.1 $\nu_3 + \nu_1$
472.7	$\nu_2 + \nu_1$	785.0 $\nu_3 + 2\nu_1$

^a Obtained at ca. 80 K as a KClO_4 disk with 676.4-nm excitation. ^b Obtained at ca. 80 K as a CsI disk with 488.0-nm excitation, after exposure to moist air.

illustrated in Figures 2–8. In most cases bands attributable to the $\nu(\text{Pt-N})$ stretching mode and some ligand modes have also been observed. The appearance of these subsidiary progressions is probably due to slight geometric rearrangements of the ligands associated with the transfer of electrons along the chain.⁴

The spectroscopic constants ω_1 and x_{11} have been calculated from the wavenumbers of the bands in the observed progressions. The results from the present data are listed in Table I. The progression-forming mode behaves nearly as a simple harmonic oscillator in most cases with an average anharmonicity constant, x_{11} , of -0.48 ± 0.14 cm^{-1} .

Infrared Spectra

The IR spectra of the complexes in the region 200–450 cm^{-1} show some absorption bands at 273 m, 283 m, 351 s, and 391 s cm^{-1} for the chloride, 233 m, 272 m, and 388 s cm^{-1} for the

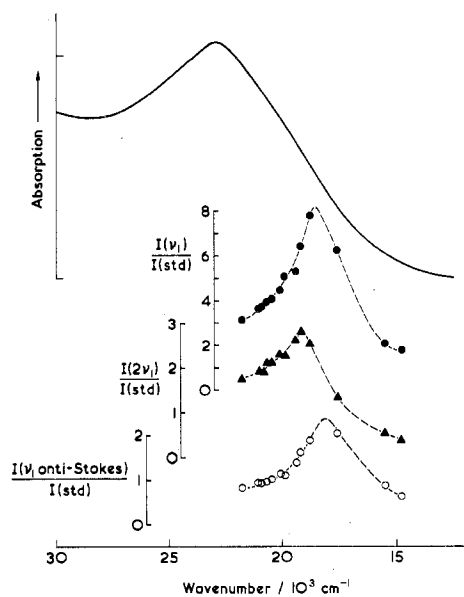


Figure 9. Electronic spectrum and excitation profiles of the Stokes ν_1 (●), Stokes $2\nu_1$ (▲), and anti-Stokes ν_1 (○) bands of $[\text{Pt}(\text{tn})_2][\text{Pt}(\text{tn})_2\text{Cl}_2](\text{ClO}_4)_4$ in KClO_4 .

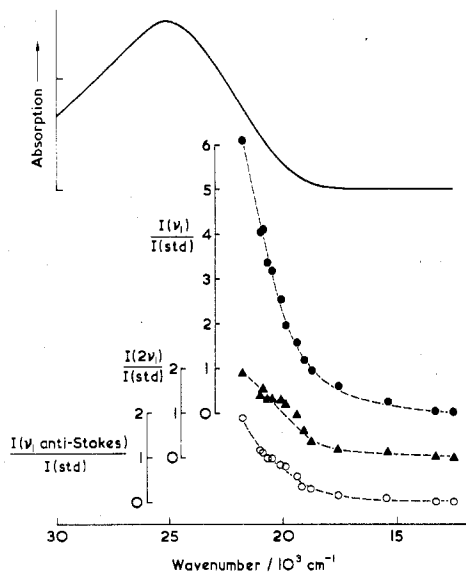


Figure 10. Electronic spectrum and excitation profiles of the Stokes ν_1 (●), Stokes $2\nu_1$ (▲), and anti-Stokes ν_1 (○) bands of $[\text{Pt}(\text{tn})_2][\text{Pt}(\text{tn})_2\text{Cl}_2](\text{ClO}_4)_4$ in CsCl , after exposure to moist air.

bromide, and 285 s, 226 m, and 187 w cm^{-1} for the iodide. The bands at 351, 232, and 187 cm^{-1} are assigned to the $\nu_{\text{as}}(\text{Pt}-\text{Cl})$, $\nu_{\text{as}}(\text{Pt}-\text{Br})$, and $\nu_{\text{as}}(\text{Pt}-\text{I})$ mode, respectively. These bands are also observed in the Raman spectra but are weak.

Excitation Profiles

Excitation profiles (EP) have been recorded at room temperature for all the perchlorate salts, in two matrices, either KClO_4 or K_2SO_4 and the appropriate alkali halide. In the case of the alkali halide matrices, the complexes were ground with the alkali halide until no further color changes were observed and then mixed with the standard, KClO_4 or K_2SO_4 . In the other case the complexes were mixed with the standard only. The excitation profiles are shown in Figures 9–14 together with the electronic transmission spectra at room temperature in the appropriate disk. The maxima of the EP's for the Stokes ν_1 band are listed in Table I for each complex. The excitation profiles for both the Stokes and anti-Stokes ν_1 bands maximize on the low-energy side of the electronic band maxima, except

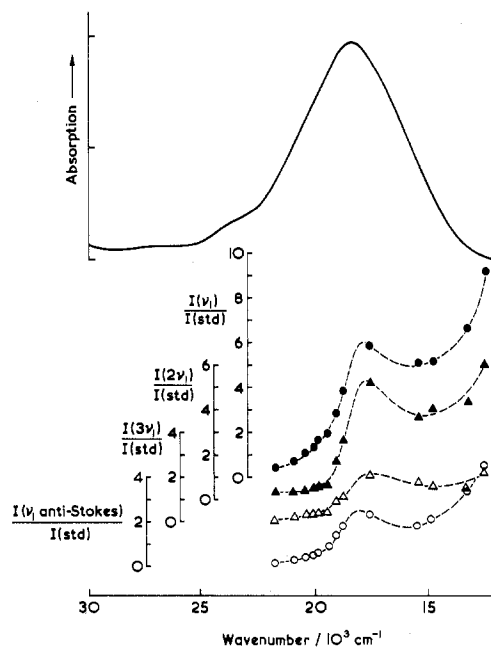


Figure 11. Electronic spectrum and excitation profiles of the Stokes ν_1 (●), Stokes $2\nu_1$ (▲), Stokes $3\nu_1$ (Δ), and anti-Stokes ν_1 (○) bands of $[\text{Pt}(\text{tn})_2][\text{Pt}(\text{tn})_2\text{Br}_2](\text{ClO}_4)_4$ in KClO_4 .

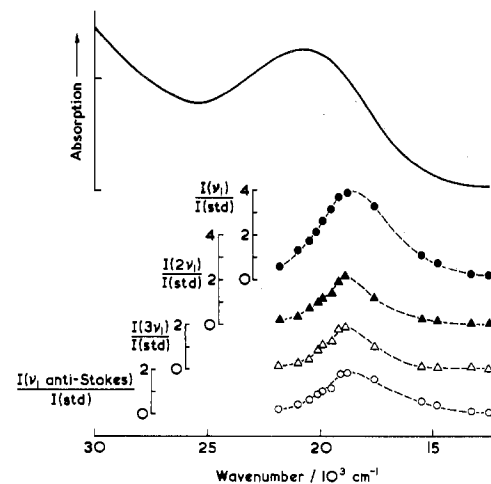


Figure 12. Electronic spectrum and excitation profiles of the Stokes ν_1 (●), Stokes $2\nu_1$ (▲), Stokes $3\nu_1$ (Δ), and anti-Stokes ν_1 (○) bands of $[\text{Pt}(\text{tn})_2][\text{Pt}(\text{tn})_2\text{Br}_2](\text{ClO}_4)_4$ in KBr , after exposure to moist air.

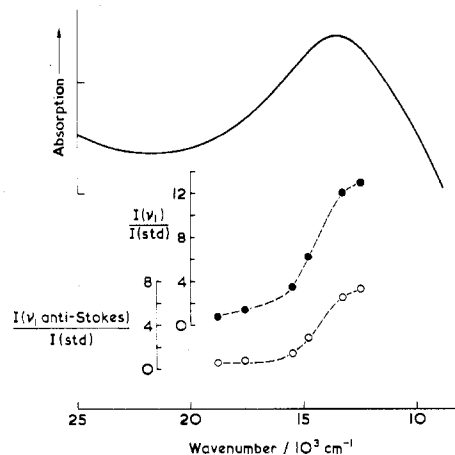


Figure 13. Electronic spectrum and excitation profiles of the Stokes ν_1 (●) and anti-Stokes ν_1 (○) bands of $[\text{Pt}(\text{tn})_2][\text{Pt}(\text{tn})_2\text{I}_2](\text{ClO}_4)_4$ in KClO_4 .

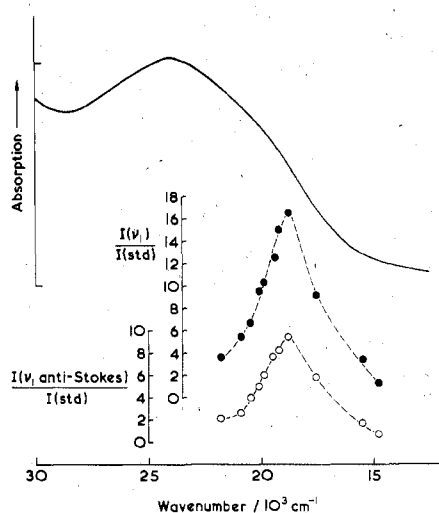


Figure 14. Electronic spectrum and excitation profiles of the Stokes ν_1 (●) and anti-Stokes ν_1 (○) bands of $[\text{Pt}(\text{tn})_2][\text{Pt}(\text{tn})_2\text{I}_2](\text{ClO}_4)_4$ in CsI, after exposure to moist air.

in the case of the bromide where a shoulder is observed at about $17\,600\text{ cm}^{-1}$ (Figure 11) and another maximum in the far-red region ($\leq 12\,500\text{ cm}^{-1}$).

Preliminary data on a Kramers–Krönig analysis of the reflectivity data indicate that the excitation profiles maximize near the maxima of the imaginary part of the dielectric constant (ϵ''), which is also the gap frequency (ω_g) in semiconductors.¹⁴

Discussion

The most remarkable feature of the RR spectra of the mixed-valence linear-chain complexes studied is the extremely intense and long observed progression in ν_1 , the symmetric stretching mode, $\nu(\text{X}-\text{Pt}^{\text{IV}}-\text{X})$, involving the bridging halogen atoms. The spectra are very similar to those of other mixed-valence linear-chain complexes,¹⁻⁷ implying that the resonant electronic transition is the intervalence $\text{Pt}^{\text{IV}}(d_z) \leftarrow \text{Pt}^{\text{II}}(d_z)$ band. The spectra show that the complexes still consist of the linear $\text{X}-\text{Pt}^{\text{IV}}-\text{X} \cdots \text{Pt}^{\text{II}}$ structure, even when ground in any matrix.

The crystal transmission spectrum of any of the complexes differs substantially from that of a powdered form of the sample, owing to the differing relative importance of specular vs. diffuse reflectance in the two situations.^{6,15} Moreover, the color of any given complex in its powdered form is not changed on grinding of the complex with a suitable disk material (KClO_4 , K_2SO_4 , or anhydrous alkali halide) and on then pressing the disk. In consequence, the RR spectrum of any given salt in one matrix is identical, within experimental error, with that in another; thus the RR band wavenumbers (Tables I–IV) are listed for one matrix material only (usually for that which contains the same anion as that of the mixed-valence complex).

Despite the comments above, there is a striking color change to all the alkali halide disks of these complexes on their being exposed to air (Table I). This color change is undoubtedly associated with pickup by the complex in each case of water (appearance of infrared band at $3400\text{--}3500\text{ cm}^{-1}$); this color change is reversed by heating the disk in an oven at $110\text{ }^\circ\text{C}$, and it is associated with the disappearance of the infrared band referred to above. The RR spectra of the aquated forms of complexes in alkali halide disks (Tables II–IV) differ from those of the anhydrous forms, but nevertheless it is certain that, from the appearance of the long progressions in ν_1 , the

$\text{Pt}^{\text{II}} \cdots \text{X}-\text{Pt}^{\text{IV}}-\text{X} \cdots \text{Pt}^{\text{II}}$ chains remain as the key structural feature of all forms of the complexes.

It seems probable that the effect of water vapor on alkali halide disks of the complexes is to alter substantially the nature of the hydrogen bonding present and, in consequence, the $\text{Pt}^{\text{II}} \cdots \text{Pt}^{\text{IV}}$ chain distances and intervalence transition energies. It is, for instance, already known that BF_4^- and (to a lesser extent) ClO_4^- assist in linking the Pt^{II} and Pt^{IV} atoms by hydrogen bonding to the NH_2 groups on the different platinum atoms.^{16,17} Thus for the complex $[\text{Pt}(\text{tn})_2][\text{Pt}(\text{tn})_2\text{Br}_2]\text{Y}_4$ replacement of BF_4^- by ClO_4^- as counterion leads to an increase of 0.04 \AA in the $\text{Pt}^{\text{II}} \cdots \text{Pt}^{\text{IV}}$ distance and to an increase in the wavenumber of the intervalence band of $\sim 4000\text{ cm}^{-1}$ (Table I); this suggests that the platinum atoms are more nearly equivalent with BF_4^- than with ClO_4^- as counterions and that hydrogen bonding affects significantly both the $\text{Pt}^{\text{II}} \cdots \text{Pt}^{\text{IV}}$ distances as well as the intervalence transition energies. Water molecules on diffusing into alkali halide disks may destroy the very specific hydrogen bonding between amine and ClO_4^- or BF_4^- ^{16,17} and thus lead (presumably) to a lengthening of the $\text{Pt}^{\text{II}} \cdots \text{Pt}^{\text{IV}}$ distances and (as observed, Table I) to an increase in the intervalence transition energy.

Large and surprising as these effects of water on the spectroscopic properties of the complexes are, similar differences have been observed previously between hydrated and anhydrous forms of Reihlen's green $[\text{Pt}^{\text{II}}\text{etn}_4][\text{Pt}^{\text{IV}}\text{etn}_4\text{Br}_2] \cdot \text{Br}_4 \cdot x\text{H}_2\text{O}$, where $\text{etn} = \text{ethylamine}$ and $x = 4$ or 0 .³ The hydrated form (green crystals, electronic maximum (powdered sample), $18\,250\text{ cm}^{-1}$) differs strikingly from the anhydrous form (orange crystals, electronic maximum (powdered sample), $23\,600\text{ cm}^{-1}$),^{3,6} and the $\text{Pt}^{\text{II}} \cdots \text{Pt}^{\text{IV}}$ chain distance is smaller in the former (5.586 \AA)¹⁸ than in the latter (6.095 \AA).¹⁹ Moreover, in the former, the $\text{Pt}-\text{Br}$ distances are at least 0.07 \AA more nearly equivalent than in the latter. It is also relevant that for the 1,2-diaminopropane (pn) complexes $[\text{Pt}^{\text{II}}(\text{pn})_2][\text{Pt}^{\text{IV}}(\text{pn})_2\text{I}_2]\text{Y}_4$ ($\text{Y} = \text{ClO}_4^-$ or I^-) the $\text{Pt}^{\text{II}} \cdots \text{Pt}^{\text{IV}}$ chain distance for the perchlorate salt (5.726 \AA)¹⁶ is 0.044 \AA shorter than for the iodo salt (5.770 \AA),¹⁷ consistent with the strong hydrogen bonding between the ClO_4^- ion and the coordinated amines on each platinum atom. Thus the effects of hydrogen bonding by water molecules to the coordinated amines, on chain properties of these complexes, are substantial.

The specular reflectance and RR spectra of single crystals show the one-dimensionality of the complexes. The excitation profiles of the ν_1 bands invariably reach a maximum several thousand wavenumbers to the low-energy side of the intervalence band, but the reason for this has yet to be established. The great intensity of the progression in ν_1 observed under resonance conditions provides a sensitive and rapid method of detecting new mixed-valence linear-chain complexes of this sort.

Acknowledgment. The authors are indebted to the Science Research Council and the University of London for financial support and to Johnson-Matthey Ltd. for a loan of chemicals. M.K. would like to thank the Department of Chemistry, University College, London, for a studentship. The authors also thank Drs. D. Bloor and R. Kennedy for the specular reflectance measurements.

Registry No. $[\text{Pt}(\text{tn})_2][\text{Pt}(\text{tn})_2\text{Cl}_2](\text{ClO}_4)_4$, 67844-72-8; $[\text{Pt}(\text{tn})_2][\text{Pt}(\text{tn})_2\text{Br}_2](\text{ClO}_4)_4$, 67758-24-1; $[\text{Pt}(\text{tn})_2][\text{Pt}(\text{tn})_2\text{Br}_2](\text{BF}_4)_4$, 67844-73-9; $[\text{Pt}(\text{tn})_2][\text{Pt}(\text{tn})_2\text{I}_2](\text{ClO}_4)_4$, 67825-26-7.

(16) Breer, H.; Endres, H.; Keller, H. J.; Martin, R. *Acta Crystallogr., Sect. B* **1978**, *B34*, 2295.

(17) Endres, H.; Keller, H. J.; Martin, R.; Traeger, U.; Novotny, N. *Acta Crystallogr., Sect. B* **1980**, *B36*, 35.

(18) Brown, K. L.; Hall, D. A. *Acta Crystallogr., Sect. B* **1976**, *B32*, 279.

(19) Endres, H.; Keller, H. J.; Keppler, B.; Martin, R.; Steiger, W.; Traeger, U. *Acta Crystallogr.*, in press.

(15) Papavassiliou, G. C.; Zdsitsis, A. D. *J. Chem. Soc., Faraday Trans. 2* **1980**, *76*, 104.